Optimum performance of link adaptation in HIPERLAN/2 Networks

Sébastien Simoens, Diego Bartolomé

Motorola Labs Paris, Saint-Aubin 91193 Gif-sur-Yvette France - tel: +33 (0)1 69 35 25 18

E-mail: simoens@crm.mot.com

Abstract

In this paper, link adaptation is investigated in the HIPERLAN/2 context. It is shown that updating modulation and coding on a frame basis can bring a gain theoretically greater than 2.5 dB over optimum long term approach. The influence of the small-scale fading properties in the various propagation environments and of the transmit and receive filters selectivity is studied. The throughput performance is computed both analytically and by network simulations, assuming constant interference and constant transmit power, as well as perfect knowledge of the SNIR or PER. Finally, throughput loss resulting from PER estimation errors is illustrated by simulations and sub-optimum method better suited to implementation is presented.

I. Introduction

Currently, broadband Wireless Local Area Networks (WLAN) are being standardized in Europe (ETSI BRAN HIPERLAN/2), the USA (IEEE802.11a) and Japan (ARIB MMAC HiSWAN). All these systems are nearly harmonized at the physical layer, which is based on Orthogonal Frequency Division Multiplexing (OFDM) [1]. This paper focusses on HIPERLAN/2 but some results can be extended to other OFDM based WLANs.

In HIPERLAN/2 [3], seven transmission modes are defined ranging from (BPSK, code rate 1/2) to (64QAM, code rate 3/4) providing data rates of 6 to 54 Mbit/s. The principle of link adaptation [4] is to adapt the data rate to the fluctuating link quality in order to achieve one or several performance criteria, like system throughput maximization, possibly under Quality of Service (QoS) constraints such as PDU Error Rate (PER) or maximum packet delay requirements.

In [9], the throughput on top of the physical layer is maximized by updating the mode "at a time interval significantly larger than the MAC frame duration (e.g. 5-10 MAC frames)". The problem with this strategy is that the mode update implicitly relies on the knowledge of very long term average Signal to Noise plus Interference Ratio (SNIR) or PER, which is incompatible with a mode update rate of 5-10 frames or even longer. Thus the performance bound announced in [9] is hardly attainable with the proposed strategy.

We show in this paper that, under some assumptions, a higher throughput bound can be reached by updating the mode very frequently (ideally every MAC frame, as in [5]). This strategy is based on "momentary link performance" which means short term SNIR or PER estimates, and also a priori knowledge of momentary PER vs momentary SNIR performance curves. Simulations show that the gain over ideal long term strategy can exceed 2.5 dB. Contrary to [4], the power control is not integrated to the link adaptation method, and is assumed to react only to slow variations of the propagation characteristics like path loss and shadowing. Anyway power control in HIPERLAN/2 has limited dynamic range, especially in the downlink.

In order to be able to predict the theoretical improvement, the statistical properties of small-scale fading in typical propagation environments are characterized, taking into account the influence of transmit and receive filters. The throughput performance is computed both analytically and by network simulations, assuming constant short term interference power and long term average received power, as well as perfect knowledge of the SNIR or PER. Finally, implementation in a more general context is discussed. More realistic suboptimum approaches are presented and the throughput loss is illustrated by simulations.

This paper is organized as follows. Section II analyzes the SNIR fluctuations and presents the assumptions of the study. In section III, the impact of fast fading on PER is characterized. In section IV, the analytical expression of the throughput bounds for short term and long term strategies is derived. Finally, in section V, the influence of implementation restrictions is discussed.

II. Analysis of the SNIR fluctuations

In order to derive and assess the performance of a link adaptation method, an accurate modeling of the SNIR fluctuations in a HIPERLAN/2 receiver is required. This is the purpose of this section, with an emphasis on small-scale fading statistics.

0-7803-6728-6/01/$10.00 ©2001 IEEE.

II.1. Components of the SNIR

The SNIR fluctuations are due to transmit power variations, changes in the attenuation due to propagation and variations of the interference power. In this section, we focus on variations due to small-scale (or fast) fading. As mentioned in section I, uplink power control is assumed to react only to slow variations of the propagation like path loss and shadowing, evolving on hundreds of MAC frames when small-scale fading changes significantly during a frame interval. Anyway, the uplink power control only affects the area close to the Access Point (AP) and, from a certain distance, the Mobile Terminal (MT) must transmit at full power to be able to operate in the largest possible set of modes. The same holds true for downlink power control whose dynamic range is even more restricted. For simplicity, we do not take interference fluctuations into account, although this is not a negligible phenomenon. Interference depends on many parameters, like the traffic in adjacent cells, the adjacent channel rejection, etc. In the following noise and interference power are assumed constant (isolated cell scenario).

At pedestrian speed ($v < 3m/s$) and 5 GHz center frequency, the channel coherence time is longer than 10 ms or 5 MAC frames. Therefore, we will assume in the following that the channel remains constant over the successive OFDM symbols which form a burst. The received power averaged over a burst is constant, but changes from a MAC frame to the next due to motion in a multipath environment. This fluctuation corresponds to small-scale (or fast) fading [7], the effect of which is superimposed on that of pathloss and shadowing.

II.2. Small scale fading in HIPERLAN/2

In HIPERLAN/2, complex samples are generated at $\frac{1}{T} = 20$ MHz ($T = 50ns$), which is also the bandwidth allocated to a cell. The channel model adopted [2] corresponds to the Wide Sense Stationary Uncorrelated Scatterers (WSSUS) model. The tapped delay line has a resolution of T_c =10 ns which is 5 times shorter than T. The impulse response at time t can be modeled as:

$$h_{ch}(\tau,t) = \sum_{i=0}^{I-1} \alpha_i(t)\delta(\tau - iT_c) \quad (1)$$

where each coefficient α_i is also a complex independant gaussian process of variance P_i such that $\sum(P_i) = 1$. Denoting by $h_{tx}(\tau)$ (resp $h_{rx}(\tau)$) the transmit (receive) filters, the overall filter $h_o(\tau,t) = h_{tx}(\tau) \star h_{ch}(\tau,t) \star h_{rx}(\tau)$ has a passband of $\frac{1}{T}$ if filters are selective enough. Thus $h_o(\tau,t)$ can be represented as a T-spaced tapped delay line. For instance, a basic transmit filter is a zero-order hold of duration T which models the D/A converter. Assuming that the A/D converter bandwidth is much larger than 20 MHz, the overall filter has $J < I$ coefficients:

$$h_o(\tau,t) = \sum_{i=0}^{J-1} \gamma_i(t)\delta(\tau - iT) \quad (2)$$

where $\gamma_i(t) \triangleq \sum \alpha_j(t)/round(jT_c) = iT$. With the zero-order hold filter, the $\gamma_i(t)$ are also complex independant gaussian processes of variance Q_i such that $\sum(Q_i) = 1$.

Within the $\frac{1}{T}$ bandwidth, the OFDM spectrum is almost flat (except at band edges) and it is also well known that the time domain samples exhibit complex gaussian distribution. Therefore, in the following the transmitted OFDM signal is modeled as complex AWGN of variance P_s. Denoting $x(n)$ the transmitted signal, the received signal is $y(n) = \sum_{i=0}^{J} \gamma_i(n)x(n-i)$. The average received power in a burst is thus:

$$P_{burst} = E\left[|y(n)|^2\right] \quad (3)$$

$$= \sum_{i=0}^{J-1} |\gamma_i|^2 E\left[|x(n-i)|^2\right] \quad (4)$$

$$= P_s \sum_{i=0}^{J} |\gamma_i|^2 \triangleq PsF \quad (5)$$

We define the fast fading F as the fluctuation of the average received power. F is a sum of independant chi-squared variables of variance Q_i such that $\sum(Q_i) = 1$.

Note that on a given sub-carrier, the frequency domain channel coefficients are complex gaussian (because the γ_i are complex gaussian and the DFT is a linear operation) and the power is chi-squared. The fluctuation of F will be less important than that of a chi-squared distribution, as illustrated on figure 1. This result is to be related to [7], in which the fading obtained by broadband sounding fluctuates less than that obtained with narrowband sounding. In the special case when $Q_i = 1/J \ \forall i$, the distribution of F turns out to be a chi-squared with $2J$ degrees of freedom.

On figure 2, the fast fading distribution of two typical HIPERLAN/2 channel models is represented. Channel model 'A' corresponds to a typical office environment, with exponentially decaying power delay profile and 50 ns RMS delay spread. Although it is described by 18 taps spaced by 10 ns each other, the Probability Density Function (PDF) matches very closely that of a chi-squared with only 6 degrees freedom. Channel model 'C' is typical of large open spaces and has a longer rms delay spread (150 ns). Moreover its power delay profile is flatter than that of model 'A'. Therefore, it matches a chi-squared with 16 degrees freedom. At 5% PDF, the range of F is $\pm$4.5 dB for channel 'A' and $\pm$3 dB for channel 'C'. This means that there are less fluctuations on channel 'C' than on channel 'A'.

In a realistic system, transmit and receive filters will have to be more selective, to be compliant with respectively the

transmit spectrum mask and the Adjacent Channel Rejection specification. Thus, their impulse response will be longer than T. Clearly, this will further combine multipath components and reduce the degree of the observed fading (or equivalently increase its variance).

III. Effect of small-scale fading on PER performance

The previous section dealt with the modeling of SNIR fluctuations and especially small-scale fading. Prior to the derivation of link adaptation performance, the effect of the PDF of the small-scale fading on PER has to be analyzed. This is what is investigated in this section, along with the definition of momentary PER and momentary SNIR with respect to average PER and SNIR.

The PER in a HIPERLAN/2 burst is a function of the channel and the noise denoted by random vectors $\mathbf{n}$ and γ. For a given channel model, the average PDU Error Rate $\overline{PER}$ only depends on $\overline{SNIR} = \frac{P_s}{\sigma_n^2}$, which is the average SNIR:

$$\overline{PER}\left(\frac{P_s}{\sigma_n^2}\right) = E\left[PER_{burst}(\mathbf{n},\gamma)\right] \quad (6)$$

$$= E\left[\int_{F=0}^{+\infty} PER_{burst}\left(\mathbf{b},\gamma\middle|\sum_{i=0}^{J-1}|\gamma_i|^2 = F\right)p(F)dF\right] \quad (7)$$

$$= \int_{F=0}^{+\infty} E\left[PER_{burst}\left(\mathbf{b},\gamma\middle|\sum_{i=0}^{J-1}|\gamma_i|^2 = F\right)\right]p(F)dF \quad (8)$$

The term $E\left[PER_{burst}\left(\mathbf{b},\gamma\middle|\sum_{i=0}^{J-1}|\gamma_i(n_{burst})|^2 = F\right)\right]$ corresponds to the expectation of the PER in a burst when only the fast fading is known (i.e. when the SNIR in the burst is known). Therefore we denote it by $PER_m\left(\frac{FP_s}{\sigma_n^2}\right)$, standing for momentary PDU Error Rate. Likewise, the SNIR in the burst is called momentary SNIR $SNIR_m \triangleq \frac{FP_s}{\sigma_n^2}$. The PER_m vs $SNIR_m$ performance is estimated by transmitting a large number N_{burst} of bursts, each containing $N_{LCH} \geq 1$ LCH PDU, and multiplying every channel coefficient $\gamma_i(n_{burst})$ by $\sqrt{\frac{F}{\sum_{i=0}^{J-1}|\gamma_i(n_{burst})|^2}}$. A traditional method to estimate $\overline{PER}$ is to transmit many bursts in order to obtain as many trials as possible for the channel and noise processes. However, another method is to estimate PER_m vs $SNIR_m$ first and derive $\overline{PER}$ vs $\overline{SNIR}$ by taking the expectation of PER_m with respect to F as described in equation (8). This is illustrated by figure 3. On this figure, the dashed curve corresponds to $PER_m\left(\frac{FP_s}{\sigma_n^2}\right)$ and the solid curve represents the average PER ($\overline{PER}$). The dotted curve is the prediction of $\overline{PER}$ from PER_m, using the PDF curve of figure 1. It can be verified that prediction and observation match very precisely.

In order to analyze into more details the relationship between PER and small-scale fading, let us consider how the HIPERLAN/2 system is specified. HIPERLAN/2 implements a bit-interleaved convolutionally coded modulation of bursts. It can be verified [6] that a convolutionally coded transmission over a flat-fading Rayleigh channel associated to Viterbi decoding at the receiver has an equivalent diversity order equal to d_{free}, the free distance of the code. In HIPERLAN/2, $d_{free} = 10$ (without puncturing). Thanks to the DFT properties, one can verify that:

$$F = \sum_0^{J-1}|\gamma_i|^2 = \sum_0^{N-1}|h_o(i)|^2 = \frac{1}{N}\sum_0^{N-1}|H_j|^2 \quad (9)$$

Where H_k $k = 0..K-1$ are the frequency domain channel coefficients on the K useful subcarriers. The decoding process behaves like taking a decision on a combination of the diversity branches, each having a complex gain equal to a frequency interleaved channel coefficient. Thus the signal to noise ratio of the decision variable is tiself a random variable of expectation of $\frac{FP_s}{\sigma_n^2}$. Which shows the direct relationship between $\overline{PER}$ and F.

IV. Ideal link adaptation

The theoretical throughput offered by the PHY layer depends on the selected PHY mode and on the PER. In this section, the throughput is approximated by $r(1-PER)$ for a nominal bit rate r. This assumption will be further discussed in section V.

When the nominal data rate r is fixed for the duration of a connection, the average throughput only depends on $\overline{SNIR}$ and is given by $\overline{\rho}^r \approx r(1-\overline{PER})$. The PHY mode associated to the highest throughput can be selected from figure 4. which is derived from $\overline{PER}$ vs $\overline{SNIR}$ link simulations as those provided in [3]. This is the procedure proposed in [9] and [8]. The average throughput with this strategy is:

$$\overline{\rho}_{long}(\overline{SNIR}) = \mathrm{Max}_{r=6,\ldots,54Mbps}\left(r\left(1-\overline{PER}^r(\overline{SNIR})\right)\right) \quad (10)$$

$$= \mathrm{Max}_r\left(\int_{F=0}^{+\infty} r(1-PER_m^r(SNIR_m))\,p(F)dF\right) \quad (11)$$

As stated in section I, the condition to reach the throughput bound $\overline{\rho}_{long}$ is that $\overline{SNIR}$ remain constant and be perfectly estimated. At pedestrian speed, this requires an estimation on thousands of MAC frames, which is a problem because path loss and shadowing are likely to evolve over such a period.

The long term throughput can be increased if the PHY mode is changed frequently (say every frame). In this case, knowing $SNIR_m$, the PHY mode maximizing the momentary throughput is selected:

$$\rho_m^{max}(SNIR_m) = \mathrm{Max}_{r=6,\ldots,54Mbps}\left(r\left(1-PER_m^r(SNIR_m)\right)\right) \quad (12)$$

If $SNIR_m$ of the next frame can be perfectly predicted, then the average throughput is maximized:

$$\overline{\rho}_{short} \approx \int_{F=0}^{+\infty} \rho_m^{max}\left(SNIR_m = \frac{FC}{I}\right) p(F)dF > \overline{\rho}_{long} \tag{13}$$

Figure 5 presents some simulation results obtained using the Network Simulator (NS) software environment. The parameters are: 1 Access Point, 1 Mobile Terminal (MT), full load, 100% uplink traffic (unacknowledged), connection duration of 10s (5000 MAC frames), BRAN-A channel model, 2 m/s speed. The MT is far enough so that it always transmits at full power (no influence of uplink power control). Dotted and solid curves represent $\overline{\rho}_{short}$ and $\overline{\rho}_{long}$ obtained resp. from equation (13) and (11). On dashed curve, the mode of each frame is decided based on the $SNIR_m$ estimated perfectly on the previous frame. Short term link adaptation simulation and analytical computation of theoretical bound match well. This confirms that the proposed short term approach outperforms ideal long term by up to 2.5 dB. It can be verified that

- The gain $\overline{\rho}_{short} - \overline{\rho}_{long}$ increases with the variance of F. This means the gain will be larger with more realistic selective filtering.
- The short term strategy will remain optimum even in the presence of path loss and shadowing, because only the knowledge of $SNIR_m$ is required. Thus, in a realistic scenario the gap between both strategies will increase.

V. Implementation issues

In the previous section, we have computed the theoretical performance of short term link adaptation strategy in the HIPERLAN/2 context. Here we review these results in the light of practical implementation constraints.

The first restriction is the fact that $SNIR_m$ estimates might be erroneous by several dBs. Interference burstiness and unpredictability is a major source of error. This is one of the reasons why in [9] it is recommended not to update the mode more frequently than every 5 or 10 MAC frames, enabling interference measurements averaging. By redefining the PER_m and SNR_m over 5 or 10 MAC frames instead of a single one, the short term strategy remains the best one.

Another restriction is due to Automatic Repeat reQuest (ARQ) specification and QoS constraints. At mode transition points, the PER_m can exceed 10% which leads to retransmissions and packet delays incompatible with real-time services. Taking a margin around these transition points where the more robust mode is systematically chosen can be a solution. Another solution is to include PER_m measurements in the decision criterion. On figure 6, the same scenario as figure 5 is used. The dashed curve represents the throughput obtained using PER_m estimate from the previous frame to decide on the mode of the current frame. The PER_m based algorithm is simple: when the PER_m is above 10%, data rate is decreased, and it can be increased again when the PER_m is below 5%. Only a slight degradation of throughput is observed. The solid curve represents a hybrid algorithm which includes both PER_m and $SNIR_m$ criteria in the decision and combines a low PER_m with a high throughput.

VI. Conclusions

In this paper, we have shown that instantaneous link adaptation performs more than 2.5 dB gain better than ideal long term link adaptation in the HIPERLAN/2 context. We have derived an analytical model for deriving the throughput of both link adaptation approaches and studied the impact of channel RMS delay spread and selective filtering. Finally we have presented sub-optimum approaches which are better suited to implementation, and compared their performance with ideal methods in a network simulation environment.

VII. References

[1] M. Alard and R. Lassale. Principles of Modulation and Channel Coding for Digital Broadcasting for Mobile Receivers. *European Broadcasting Union Review Technical*, 224:168–190, August 1987.

[2] ETSI Normalization Commitee. Channel Models for HIPERLAN/2 in different indoor scenarios. Norme ETSI, document 3ERI085B, European Telecommunications Standards Institute, Sophia-Antipolis, Valbonne, France, 1998.

[3] J. Khun-Jush, P. Schramm, U. Wachsmann, and F. Wenger. Structure and Performance of the HIPERLAN/2 Physical Layer. In *Proceedings of the IEEE VTC conference*, volume 5, pages 2667–2671, Amsterdam, Netherlands, June 1999.

[4] Kin K. Leung and Li-Chun Wang. Integrated Link Adaptation and Power Control in wireless IP networks. In *Proceedings of the IEEE VTC Fall conference*, volume 3, pages 2086–2092, September 2000.

[5] Hui Li, Göran Malmgren, Mathias Pauli, Jürgen Rapp, and Gerd Zimmermann. Performance of the Radio Link Protocol of HIPERLAN/2. In *proceedings of IEEE PIMRC*, September 2000.

[6] J. G. Proakis. *Digital Communications*. Mc Graw Hill, New York, USA, 3rd ed., 1995.

[7] T.S. Rappaport. Chap 4-Mobile Radio Propagation: Small-Scale Fading and Multipath. In Prentice-Hall, editor, *Wireless Communications, Principles and Practice*. New Jersey, 1996.

[8] Muneta S., Matsumoto Y., Mochizuki N., and Umehira M. A new frequency-domain link adaptation scheme for broadband OFDM systems. In *Proceedings of the IEEE VTC conference*, 1999.

[9] Johan Torsner and Göran Malgrem. Radio network solutions for HIPERLAN/2. In *Proceedings of the IEEE VTC conference*, volume 2, pages 1217–1221, 1999.

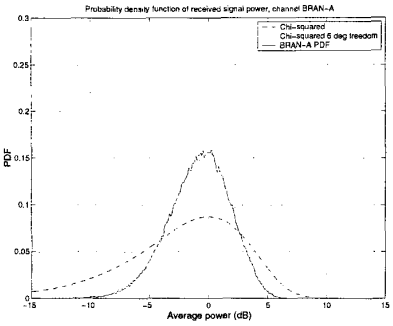

Figure 1: PDF of small-scale fading, HIPERLAN/2 channel model A

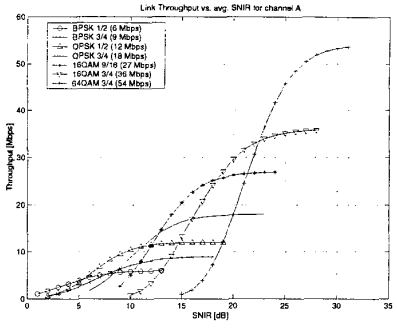

Figure 4: Long term throughput vs long term SNIR, channel model 'A'

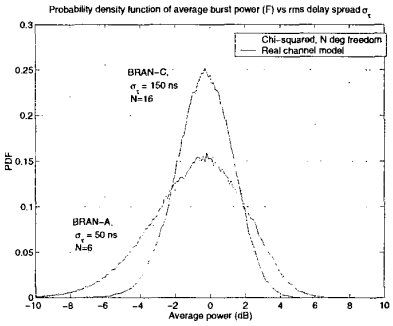

Figure 2: PDF of small-scale fading, comparison of channel A and C

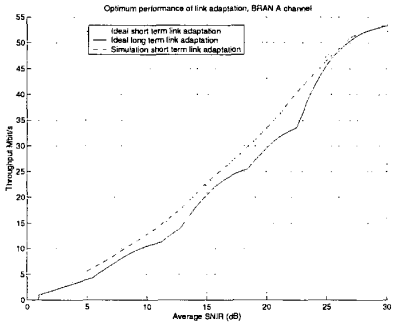

Figure 5: Performance of various link adaptation strategies

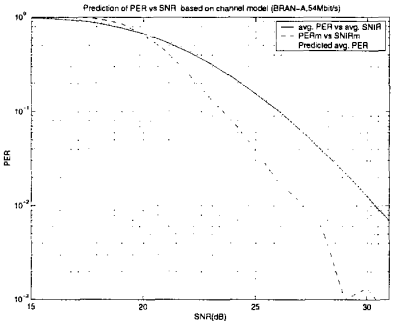

Figure 3: Prediction of $\overline{PER}(\overline{SNIR})$ from $PER_m(SNIR_m)$ curves (54Mbit/s mode, channel model 'A')

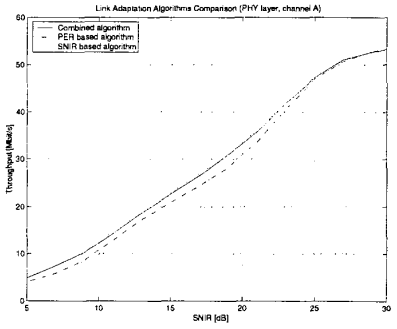

Figure 6: Performance of more robust sub-optimum link adaptation algorithms